

Article

Influence of Column–Base Connections on Seismic Behavior of Single-Story Steel Buildings

Alessandro Prota ¹, Roberto Tartaglia ^{2,*} and Raffaele Landolfo ¹

¹ Department of Structures for Engineering and Architecture, University of Naples Federico II, Via Forno Vecchio, 80134 Naples, Italy; alessandro.prota@unina.it (A.P.); landolfo@unina.it (R.L.)

² Department of Engineering (DING), University of Sannio, Piazza Roma, 82100 Benevento, Italy

* Correspondence: rotartaglia@unisannio.it

Abstract: This study focuses on assessing the seismic performance of existing single-story steel buildings used as industrial buildings. This research aims to provide a systematic procedure for evaluating the seismic response of a single-story strategic building and properly accounting for the behavior of the column–base joints. Through meticulous data collection, advanced numerical modeling, and pushover analyses, this study highlights the significant impact of column–base joint behavior on the overall seismic performance of industrial buildings. The findings reveal that while single-story steel buildings show a satisfactory seismic performance in terms of lateral resistance and stiffness in the longitudinal direction, deficiencies in the joint design can strongly impact the performance in the transversal direction. This study emphasizes the necessity of incorporating joint flexibility into numerical analyses to accurately assess structural behavior. In conclusion, a precise assessment of the base joints provides insights for informing retrofitting strategies.

Keywords: existing building; seismic assessment; steel structures; column–base joints; finite element analysis



Citation: Prota, A.; Tartaglia, R.; Landolfo, R. Influence of Column–Base Connections on Seismic Behavior of Single-Story Steel Buildings. *Buildings* **2024**, *14*, 3606. <https://doi.org/10.3390/buildings14113606>

Academic Editor: Harry Far

Received: 21 October 2024

Revised: 8 November 2024

Accepted: 11 November 2024

Published: 13 November 2024



Copyright: © 2024 by the authors. Licensee MDPI, Basel, Switzerland. This article is an open access article distributed under the terms and conditions of the Creative Commons Attribution (CC BY) license (<https://creativecommons.org/licenses/by/4.0/>).

1. Introduction

This study examines the seismic performance of six existing single-story non-residential steel buildings located in Italy and situated in various seismic zones. In Italy, steel structures became increasingly popular in the second half of the 20th century, primarily due to their ability to span large distances without the need for complex technological solutions [1]. This advantage was particularly important in an era when there was a growing demand for open, flexible spaces in industrial and commercial buildings, as well as in infrastructure projects. Steel provided a practical solution to these needs by enabling long spans and large, uninterrupted spaces, which were difficult to achieve with traditional materials. Non-residential single-story steel buildings comprise a significant portion of the Italian building stock; while their primary application has been industrial [2,3], single-story designs are also suitable for various other purposes. The primary issues that can lead to severe damage in such structures following seismic events are related to the evolution of the seismic classification and the development of regulations concerning the design criteria over time. Most of the Italian building stock consists of buildings designed only to withstand gravity loads [1]; only after the Molise earthquake in 2003 was the entire Italian territory classified as an earthquake-prone region. Moreover, the seismic performance of steel structures heavily depends on the details of their connections. In the past, the lack of a differentiation between ductile and brittle mechanisms in connection designs resulted in vulnerabilities [4]. Connections designed without considering capacity design principles are more likely to fail under seismic loads; therefore, assessing these details is a critical component of evaluating overall seismic performance.

This evaluation is particularly important for single-story steel buildings, which usually combine different lateral-force-resisting systems: braced frames in the longitudinal

direction and moment-resisting frames for the main steel frames, offering flexibility in the design and accommodating openings like doors and windows. Conventional analyses often assume either perfectly rigid or nominally pinned connections concerning the column–base connections of the main steel frames, simplifying the implementation and design procedures. However, these assumptions may need revision since most real-world joints transmit limited moments and undergo significant deformations under loads. Thus, incorporating joint flexibility into numerical analyses is necessary to assess the true behavior of a frame.

The aim of this work is to compare the seismic performance of the investigated single-story steel buildings by offering a schematic procedure for a code-compliant assessment. It emphasizes the importance of the original design typology and the effect of the column–base joint behavior, considering both the ideal fully rigid or pinned conditions and the real behavior obtained from a code-conforming simulated joint design. In the first part of the paper, six case studies located in different parts of Italy, representative of different main steel frame configurations and designed in different time periods, are presented. The procedure for obtaining information about the structural material properties and the main features of the column–base connection is then described. Following this data collection phase, refined numerical models that use component-based finite element methods are developed to define the moment–rotation response of the column–base joints. Then, global 3D non-linear numerical models of the selected case studies are developed, incorporating the previously mentioned column–base joint behaviors through the calibration of non-linear links. Pushover analyses are carried out to assess the seismic performance of these models. Finally, based on the results of the analysis, local seismic reinforcement interventions are presented.

2. Existing Strategic Single-Story Buildings

2.1. General Description

Six existing single-story non-residential steel buildings, located in different parts of Italy (IT), were selected as case studies (see Figure 1). The investigated buildings were considered strategic structures because they are involved in industries with activities that pose particular risks. These buildings are located in six different Italian provinces: Brescia (BS), Bologna (BO), Viterbo (VT), Chieti (CH), Palermo (PA), and Reggio Calabria (RC).

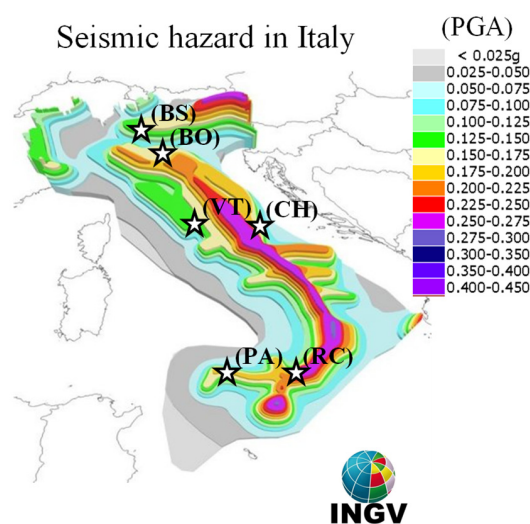


Figure 1. Location of the selected case studies.

A proper nomenclature was introduced in order to uniquely identify the investigated single-story steel buildings:

- The structural material: steel (S).
- The building's location: through the abbreviation of the Italian provinces where the buildings are located (i.e., if located in Bologna, (BO)).

Therefore, the building located in Bologna is hereafter indicated as S-BO.

All the investigated case studies are characterized by a regular rectangular plan, with a plan extension ranging from 1184 m² (for S-BS) to 450 m² (for S-CH).

Typically, in the construction of single-story steel buildings, an external cladding envelope is employed. This envelope is often upheld by secondary steel members with relatively short spans, which, in turn, rely on the primary steel structure for support. In particular, the investigated buildings present three different configurations with respect to the main steel frames (see Figure 2): (a) rigid portal frames (RPFs), (b) rigid truss frames (RTFs), and (c) pinned truss frames (PTFs). RPFs are characterized by a rigid joint (a moment-resistant connection) between the ends of the roof beams and the columns; meanwhile, in RTFs, the attainment of rigid frames involves the connection of both the top and bottom chords to the supporting columns. Finally, PTFs are characterized by a pinned connection between the ends of the roof beams and the columns, providing energy dissipation mainly at the bases of the columns.

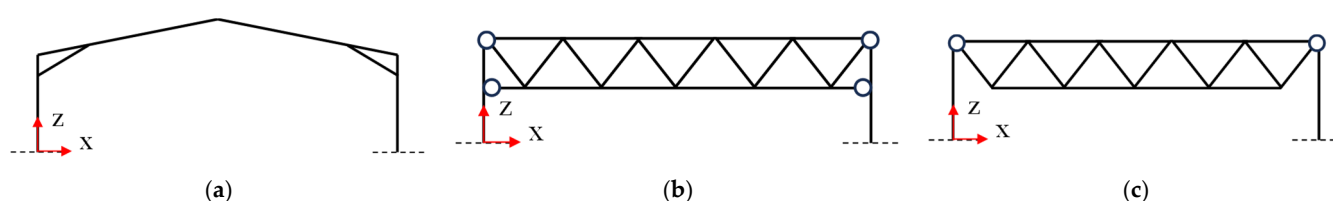


Figure 2. Main steel frame configuration: (a) RPF (S-VT); (b) RTF (-BO); and (c) PTF (S-CH).

The main steel frames provide lateral stiffness and resistance in the transverse direction (Dir. X), while in the longitudinal direction (Dir. Y), for all the investigated case studies, concentrically braced frames (CBFs) were adopted as the lateral-force-resisting systems (LFRS). As typical for non-residential steel single-story buildings, cross bracing spanning both in the longitudinal and transverse directions is employed to provide the roof diaphragm's action. Table 1 summarizes the main geometrical features and structural schemes of the examined existing buildings.

Table 1. Case studies: main features.

ID Label	Dir. X Width L_x (m)	Dir. Y Width L_y (m)	Plan Extension A (m ²)	Headroom H (m)	Dir. X LFRS	Dir. Y LFRS	N ^o Transverse Frame
S-BS	37	32	1184	6.7	RTF	CBF	8
S-VT	30	32	960	10	RPF	CBF	6
S-BO	35	30	1050	7	RTF	CBF	7
S-CH	15	30	450	7	PTF	CBF	7
S-PA	22	30	660	7.4	PTF	CBF	8
S-RC	35	30	1050	7.8	RTF	CBF	7

2.2. Information on As-Built Existing Buildings

The investigated buildings were erected within a time range that spans from 1972 to 1992. The construction periods allow us to identify the design typology adopted for the case studies based on the code in force at the time of construction [5–10] (see Table 2). Thus, until the beginning of the 1970s, two different design approaches were adopted in Italy: gravity load (GL) and obsolete seismic (OS) design. In the case of GL design, seismic action was totally neglected; in conjunction, the CNR guidelines [11,12] were widely used by Italian steel designers. These guidelines required the action of wind to be taken into account by applying equivalent pressures to structures based on a site's location. Subsequently, considering a structure's geometry, these pressures were converted into equivalent horizontal and vertical forces acting on the structure.

Table 2. Case studies: design approach and reference design codes.

ID Label	Design Year	Design Approach	Reference Design Code	Reference Seismic Code
S-BS	1980	GL	[6]	-
S-VT	1990	GL	[8]	-
S-BO	1993	GL	[8]	-
S-CH	1995	GL	[8]	-
S-PA	1975	OS	[5]	[9]
S-RC	1985	OS	[7]	[10]

Contrariwise, the OS approach was based on considering seismic action as an equivalent static horizontal force proportional to the seismic weight of the structure, defined in accordance with the old Italian regulations [9,10]. However, it should be noticed that the OS approach was adopted just for buildings located in the sites classified as within seismic zones at that time period. Indeed, only one-quarter of the country was classified as a seismic-prone region before the 1980s, whereas only after the “Puglia and Molise” earthquake was (2002) a new seismic classification, considering four different seismic zones and including the entire national territory, applied.

As concerns structural identification, the information about the overall dimensions and cross-sectional properties of the steel members contained in the original design reports and drawings turned out to be incomplete or unreliable, as is common in dealing with these types of existing structures. Therefore, the missing information was collected through a survey of the building and a campaign of in situ measurements.

Permanent non-structural loads considered were the cladding weight (0.15 kN/m^2) and, at the roof level, an additional insulation board (0.05 kN/m^2) and ballast (1.0 kN/m^2). Maintenance loads (0.50 kN/m^2), snow loads ($q_{s,k}$), and equivalent static wind loads ($q_{w,k}$) were considered as variable loads [13,14].

2.3. Material Properties

The material properties were obtained according to the usual constructive practice at the time of construction (see Table 2), as suggested by the Italian code provisions [13,14], or by referring to the codes in force at that time, as indicated in EN 1998-3 [15]. Recently, in 2021, Di Lorenzo et al. [16] proposed a methodology for identifying existing metal carpentry structures. It requires as input data only the functional destination and the exposure or importance of the construction [13], as well as the design year of the investigated building. Therefore, according to [16], for steel buildings erected between 1961 and 1990, the steel grade Fe360, which corresponds to steel grade S235 according to UNI EN 10025 [17], can be assumed. However, with this procedure, the properties referred to as the nominal/guaranteed values (e.g., the minimum values for current materials), as required by the product standards, may differ, significantly even, from the mean values typically used in the assessment of existing buildings.

In order to overcome this issue, it is possible to refer to the research carried out by da Silva et al. [18]. In particular, the authors, based on a database comprising 837 coupon tests derived from various sources, provide an average value for the yield strength ($f_{y,m}$) of S235 equal to 310 MPa, with a coefficient of variation (*C.o.V.*) equal to 0.10. Moreover, considering a Knowledge Level “KL2”, as result of the amount and quality of the information collected on the existing structures [13–15], a confidence factor (CF) equal to 1.20 is selected to take account of material variability.

Thus, a yield strength value (f_y) equal to 260 Mpa was used in the calculation of the steel members’ capacity.

2.4. Locations and Seismic Hazards

It is possible to classify the six sites as a function of the value of the maximum horizontal acceleration on rigid ground, which has a 10% probability of being exceeded in

50 years (a_g). The a_g values are, 0.144 g, 0.149 g, 0.164 g, 0.165 g, 0.172 g, and 0.270 g for Viterbo (VT), Brescia (BS), Bologna (BO), Chieti (CH), Palermo (PA), and Reggio Calabria (RC), respectively. The seismic actions on buildings were evaluated in relation to a reference period (V_R), which was obtained for each type of construction by multiplying its nominal design life (V_N) by the utilization coefficient (C_U). Given the strategic nature of the investigated structures, a value of 2.0 was adopted for the utilization coefficient, as reported by the Italian code provisions [13]. Therefore, assuming V_N is equal to 50 years, a reference period of 100 years was selected for the evaluation of the seismic action. A plain topography (topography class “T1”) and a medium soil class (stratigraphy class “C”) were assumed according to the geotechnical classification provided by the original design report for the six industrial buildings [13,19]. The European and Italian codes [13,19] outline multiple limit states (LSs) to ensure structural safety against seismic forces. Among these, the Damage Limitation (DL) LS and the Significant Damage (SD) LS are particularly pertinent for existing structures. To determine the seismic action associated with each of the limit states considered, it is possible to refer to the following expression:

$$T_R = -V_R / (\ln(1 - P_{V_R})) \quad (1)$$

where T_R is the mean return period of the seismic action employed, and P_{V_R} is the exceedance probability in V_R , selected in accordance with [13]. In particular, a P_{V_R} equal to 63% and 10% was assumed for the DL and SD limit states, respectively [13]. Therefore, earthquakes with T_R equal to 101 and 949 years were considered for the DL and SD limit states, respectively. Figure 3 depicts the elastic response spectra for the four selected sites at T_R values corresponding to the investigated limit states.

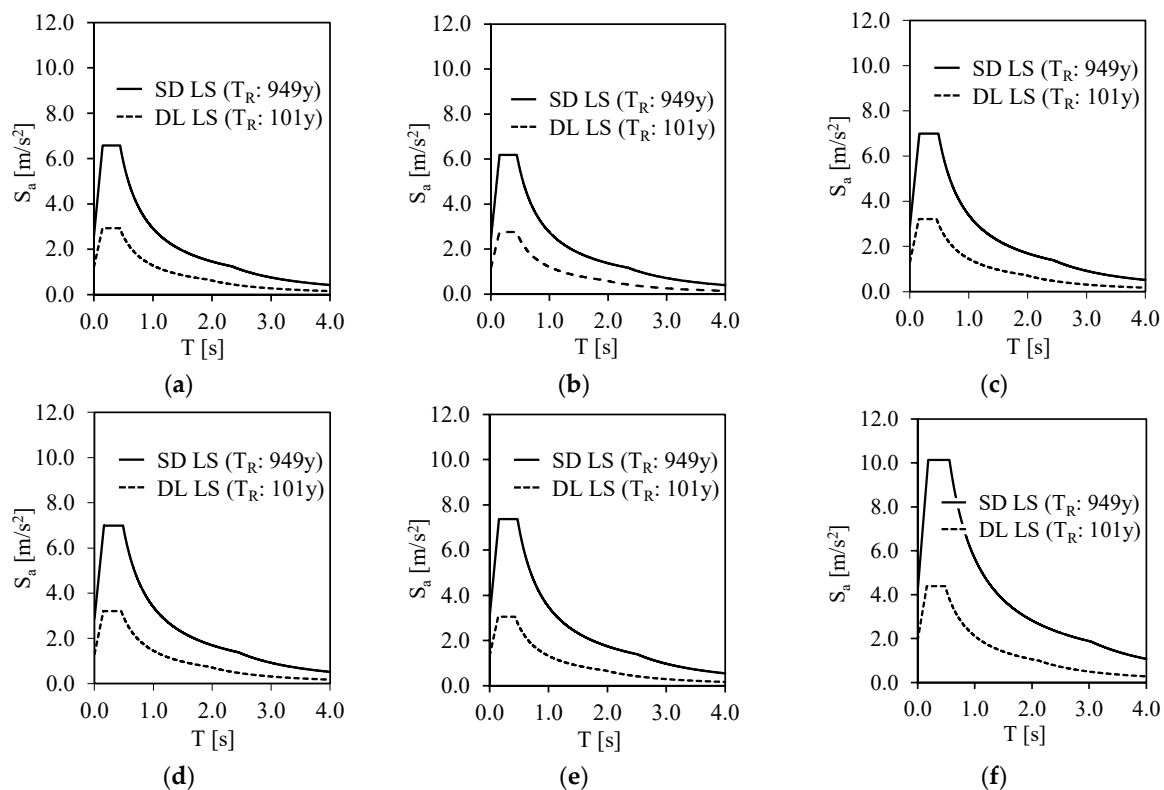


Figure 3. Elastic response spectra: (a) Brescia (BS); (b) Viterbo (VT); (c) Bologna (BO); (d) Chieti (CH); (e) Palermo (PA); and (f) Reggio Calabria (RC).

2.5. Simulated Design of the Column–Base Connections

The performance of the base connections plays a central role in the definition of single-story structures; however, in many cases, neither within the design report nor during the

visual survey is it possible to detect the details of the column–base joints. This issue is particularly relevant in the assessment of existing steel structures, in which the connections were designed just considering resistance checks, neglecting any capacity design and ductility requirements. Indeed, as reported in many post-earthquake steel building damage evaluations [20,21], several column–base connections designed following previous design practices and guidelines did not perform satisfactorily. Indeed, a common engineering practice is to assume column–base joints are ideally pinned or fully rigid; however, the assumption of a full-strength rigid joint is only an approximation of the real behavior. In reality, most joints can be classified as semi-rigid and partial-strength according to the EN1993-1-8 [22] classification. This additional flexibility, if ignored, can lead to significant errors in the evaluation of the structural response.

Within this framework, one of the primary objectives of this study is to compare the seismic response of the investigated industrial buildings considering two different joints configurations—(a) the “ideal” configuration, either fully rigid (I-F) or pinned (I-P), and (b) the “real” (R) configuration—by designing the base connection based on the regulatory requirements and technical procedures adopted at the time of construction.

Evaluations of the “real” joint behavior were made following a code-consistent simulated design approach in which, following the same procedure adopted by designers at the time, resistance checks were carried out in order to identify the main characteristics of the joint components (i.e., steel plate thickness, number of anchor rods, and anchor rod diameter). To support the simulated design, it was possible to refer to the CNR guidelines [11,12] and to the technical manual provided by D. Danieli and F. De Miranda in 1971 [23], in which construction practices related to non-residential single-story steel buildings are reported. In particular, according to [23], a 2D model was considered as a calculation model for the bending ($M_{j,Ed}$) and shear ($V_{j,Ed}$) at the base, in which for buildings designed according to the OS approach, the maximum value between the effect of the equivalent static seismic force (F_E) and wind (F_w) force was considered in the design. Meanwhile, for a building designed according to the GL approach, F_w was considered as the horizontal design load. Moreover, a plate thickness ranging from 15 mm to 20 mm was typically considered for the steel base plates, and for moment-resisting column–base joints, vertical stiffeners were required according to engineering practice [23].

S-PA and S-RC were designed according to OS design (see Table 2); however, due to the different construction periods, distinct seismic code guidelines were implemented for the design of these two industrial buildings. Indeed, from 1935 to 1975, Italy was divided into two seismic categories (I and II), plus a non-seismic zone in which buildings were designed accounting for gravity loads only. Seismic loads were applied as the equivalent lateral forces proportional to the building’s seismic mass equal to W_{Tot}/g . W_{Tot} includes the permanent load plus 1/3 of the variable loads. So, the design lateral force for S-PA could be calculated as follows:

$$F_E = C \cdot W_{Tot} \quad (2)$$

where C was equal to 0.10 and 0.07 for seismic categories I and II, respectively. Then, F_E was uniformly distributed across the different floors [9].

DM 03/03/1975 [10] introduced some basic earthquake engineering concepts into Italy for the first time, which remained unchanged until as late as 2003: (i) an innovative system for categorizing seismic zones; (ii) a site amplification effect; and (iii) the implementation of modal analysis (in lieu of equivalent static analysis), along with a design spectrum, as a methodology for earthquake-resistant building design. In particular, the horizontal force for S-RC could be evaluated as follows:

$$F_E = C \cdot R \cdot I \cdot W_{Tot} \quad (3)$$

where R was a coefficient that took into account the dynamic effects that could be fixed as equal to 1 for the sake of safety. Instead, coefficient I is an “importance factor” that was set to greater than 1 for structures destined to manage emergencies after an earthquake.

Furthermore, this force was not uniformly distributed across the different floors but rather with a reverse triangular distribution [10]. Then, the seismic force was divided among the different LFRSs in the direction investigated ($F_{E,i}$).

The equivalent horizontal force considered in the simulated design and the values of the bending moment (M_j), shear (V_j), and axial force (N_j) at the column–base joints are depicted in Table 3 for the six buildings investigated.

Table 3. Simulated design: column–base joint actions.

Case Study ID	F_w	$F_{E,i}$	M_j	V_j	N_j
-	[kN]	[kN]	[kNm]	[kN]	[kN]
S-BO	24	-	44	12	146
S-CH	24	/	102	12	67
S-BS	38	/	70	19	183
S-VT	150	/	559	91	368
S-RC	55	47	120	28	164
S-PA	29	15	106	15	96

Connections were designed just considering resistance checks, making assumptions about the base plate rigid elements and evaluating the action distributions on the bolts and/or welds. This presumption of rigidity allowed for the stress/strain characteristics of the anchor bolts and the concrete to be represented through an elastic model. The utilization of an elastic stress/strain model enabled the application of a linear analysis in ascertaining the compressive stress within the concrete beneath the plate, the tensile forces exerted on the anchor bolts, and the internal bending moments used to determine the thickness of the plate.

The main features of the designed column–base connections are depicted in Figure 4, in which it can be observed that with the exception of S-PA only, European wide flange columns were used for all the investigated structures. For S-PA, the column of the main frame was a built-up column composed of two UPN 180 profiles spaced 500 mm apart, connected by two steel plates with a thickness of 10 mm, which joined the flanges of the two UPN profiles.

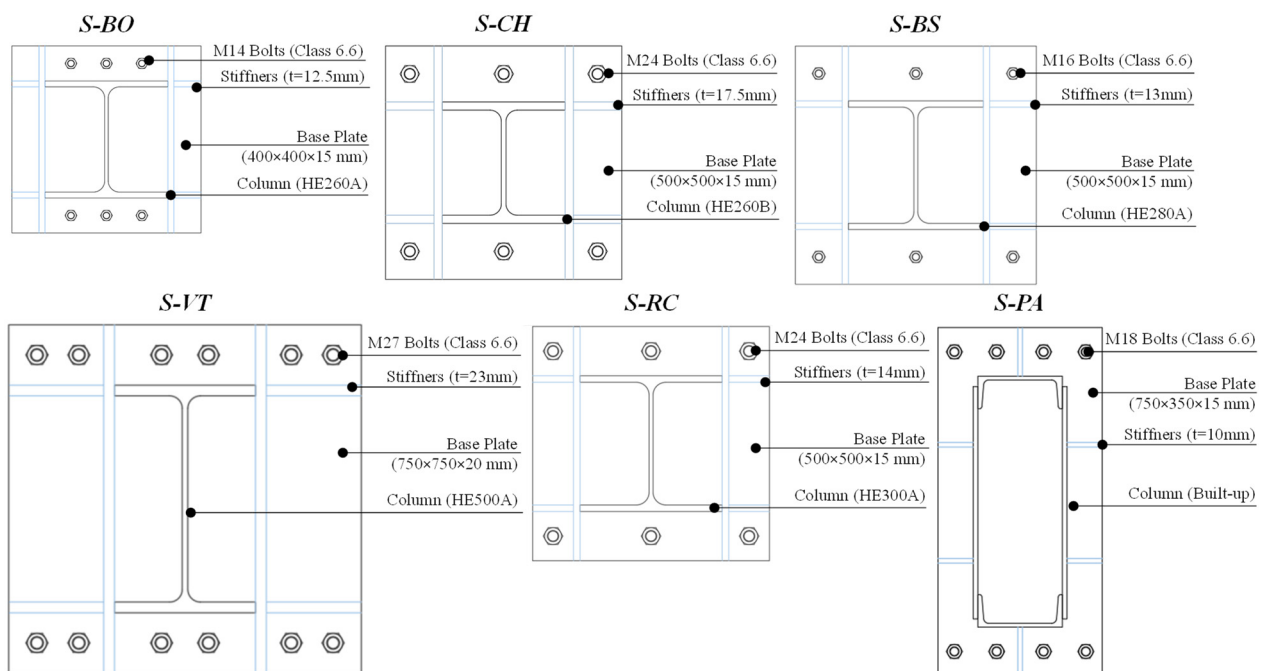


Figure 4. Main frames' column–base connection details.

3. Numerical Modeling Assumptions

3.1. Moment–Rotation Responses of the Column–Base Joints

The component method is an analytical approach, reported within EN 1993-1-8 [22], for assessing steel joint behavior. This method involves conceptualizing a joint as an assembly of distinct components, each contributing to the overall response of the joint. It should be noticed that these codified regulations are formulated assuming base plates are used without stiffeners. Nonetheless, numerous existing structures were historically designed using base plates featuring stiffeners because there were instances where local practices may have encouraged designers to persist in utilizing them. Moreover, it should be noticed that EC3 assumes constant eccentricity of the axial force, implying that an increase in the bending moment corresponds proportionally to an increase in the axial force. However, it therefore becomes crucial to assess the response of a connection in the context of a non-proportional loading path, such as a constant axial force combined with varying bending moments, as seen in assessing responses to escalating seismic loads.

The finite element method (FEM) represents a viable alternative to the component method that is able to overcome all the limits mentioned and provide a good prediction of a joint's performance; however, this method may be not suitable in terms of the modeling complexity and the computational time for field engineering. Therefore, in this study, an alternative method defined as a component-based finite element model (CBFEM) was adopted to define the moment–rotation response of the designed joints. The CBFEM is an approach that combines aspects of both the component method and the finite element method. It integrates the advantages of the component method's simplicity into analyzing joint behavior with the finite element method's ability to handle complex geometries and material behaviors.

The CBFEM breaks down a joint or connection into distinct components, similar to the component method, but it utilizes finite element techniques to analyze these individual components. Each component is modeled using finite elements, allowing for a more detailed and accurate representation of their behavior under various loads and conditions. By employing finite elements to model the components within a joint, the CBFEM enables a comprehensive analysis of complex connections, considering factors such as non-linear material behavior, geometric intricacies, and local variations in stiffness and strength. In 2023, Della Corte et al. [24] presented findings from analyses aimed at characterizing the behavior of steel column–base connections with stiffened plates. Their study demonstrated that analyses conducted using the CBFEM yielded results comparable to more detailed FE models. The designed column–base joints were modeled using IDEA StatiCa software Version 24 [25] due to its specialized focus on steel connections, utilizing the CBFEM to efficiently model complex connections with accuracy. IDEA StatiCa employs shell elements to represent the plates and specifically designed spring elements to simulate the behavior of the anchor bolts.

Therefore, 3D models of all of the investigated joints were built starting from the information summarized in Figure 5, assuming the anchor length was equal to 8 times the bolt diameter, which is the minimum length value prescribed by [22]. With respect to the concrete foundation block, its length was assumed to be equal to the depth of the anchor bolts, and the plan dimensions were set as large enough to avoid any effect of the concrete block borders on the compression resistance below the base plate.

A bilinear elastic–perfectly plastic stress/strain curve was assumed for the steel plates considering the yield strength as described in the previous section and a nominal maximum total strain equal to 0.05 [22].

Figure 5 depicts the moment–rotation response curves for all of the column–base connections investigated.

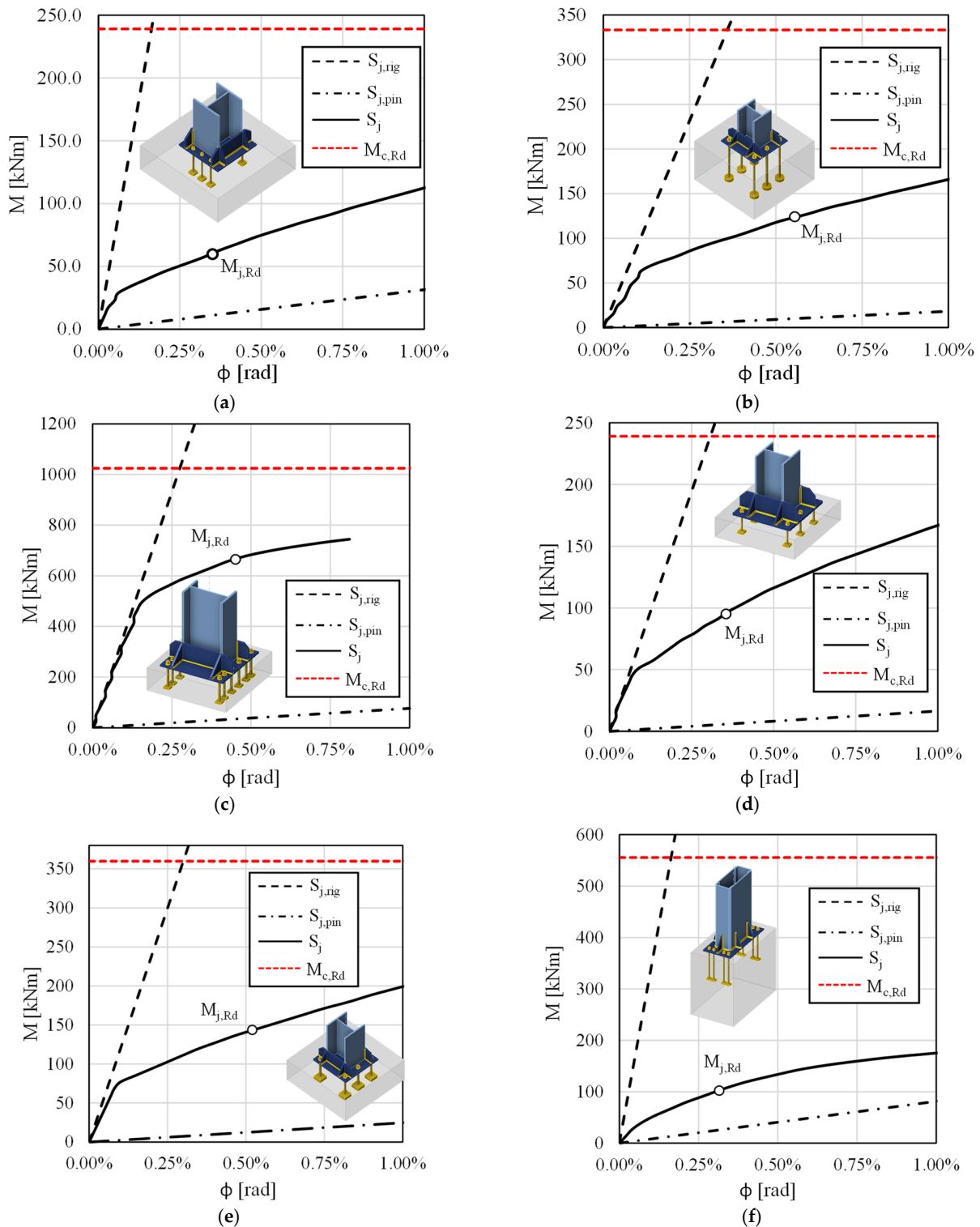


Figure 5. Moment–rotation column–base joint response curves: (a) S-BO; (b) S-CH; (c) S-BS; (d) S-VT; (e) S-RC; and (f) S-PA.

All of the joints investigated show an intermediate rotational stiffness (S_j) between that of a fixed ($S_{j,rig}$) and a hinged ($S_{j,pin}$) node and can be classified as partial rigid connections. In the same manner, comparing the joints' flexural capacity with respect to the plastic capacity of the columns ($M_{c,Rd}$), it can be observed that in none of the cases investigated, the joints show full-strength behavior; consequently, all of the joints investigated could be classified as semi-rigid and partial-strength connections in accordance with EN1993-1-8.

3.2. Assumptions of Global Finite Element Models

For the six case studies, three different sets of 3D global finite element models (FEMs) were developed in the SAP2000 environment [26] to assess the influence of the base joints on the overall behavior in the transverse direction. The aim was to evaluate how changes in the stiffness and strength of the base joints impacted the global structural response. Therefore, for each model configuration, the effects of the base joints' characteristics on the buildings' lateral performance were identified.

The first set of models was developed to assess the overall structural response while disregarding the specifics of the column–base connections, considering rigid and full-strength connections (I-R). It utilized frame elements for the beams, columns, and diagonals, representing them along the centroidal axes of the steel profiles. Due to the presence of in-plane bracing systems, a diaphragm constraint was applied at the roof level. In the PTF and RTF structures, local releases were applied to modeling the truss element connections, acting as internal hinges. To maintain flexural continuity in both the lower and upper chords, no releases were applied to these elements. The self-weight of the beams, columns, and diagonal elements was considered a dead load (G) within the model. Accounting for non-structural elements involved considering equivalent area loads: a uniform load of $g_{2k,r} = 1.2 \text{ kN/m}^2$ for the roofing system and a unitary weight of $g_{2k,c} = 0.15 \text{ kN/m}^2$ for lightweight claddings. Snow and roof maintenance live loads were included as per the Italian regulatory provisions [13].

The non-linear behavior of the steel elements was simulated using a concentrated plasticity model, placing the plastic hinges at the ends of the bending elements and in the middle of the bracing elements. The parameters adopted for the definition of the plastic hinges are in line with the guidelines set by the American Society of Civil Engineers [27].

The second set of global models mirrored the first, except for the introduction of non-linear links placed at the column–base connections (R). These links were designed to numerically characterize the behavior at the column–base joints. The plasticity model used was based on hysteretic behavior proposed by Wen [28]; it characterized the material's behavior by considering parameters that influence its stiffness, strength, and energy dissipation capabilities during cyclic loading and unloading cycles. Wen's model is valuable for simulating the plastic deformation and energy dissipation in structural elements under various loading conditions.

Calibration of these links was performed based on outcomes derived from local FEAs (see Figure 6). Table 4 showcases the parameters obtained from the last iteration of the models' calibration, where k is the elastic spring constant, $Yield$ is the yield moment, $Ratio$ is the specified ratio of post-yield stiffness to elastic stiffness (k), and exp is an exponent greater than or equal to unity (usually ranging from 1 to 20). Larger values of this exponent increase the sharpness of the yielding [26].

The third set of global models, developed for the RPF and RTF buildings, was identical to the first, with the exception that the base connection was considered to be pinned (I-P). Since a pinned base does not provide moment resistance, the system relies on the rigid connections at the beam-to-column joints, allowing the frame to act as a whole in resisting lateral forces.

Table 4. Parameters obtained from the last iteration of Wen's model calibration.

ID	Yield	k	exp	Ratio
-	(kNm)	(kNm/rad)	-	-
S-BS	47	71,000	5.0	0.24
S-VT	510	340,000	11.0	0.155
S-BO	30	57,000	2.8	0.18
S-CH	68	60,000	9.0	0.21
S-PA	78	85,750	8.0	0.18
S-RC	50	66,000	2.0	0.335

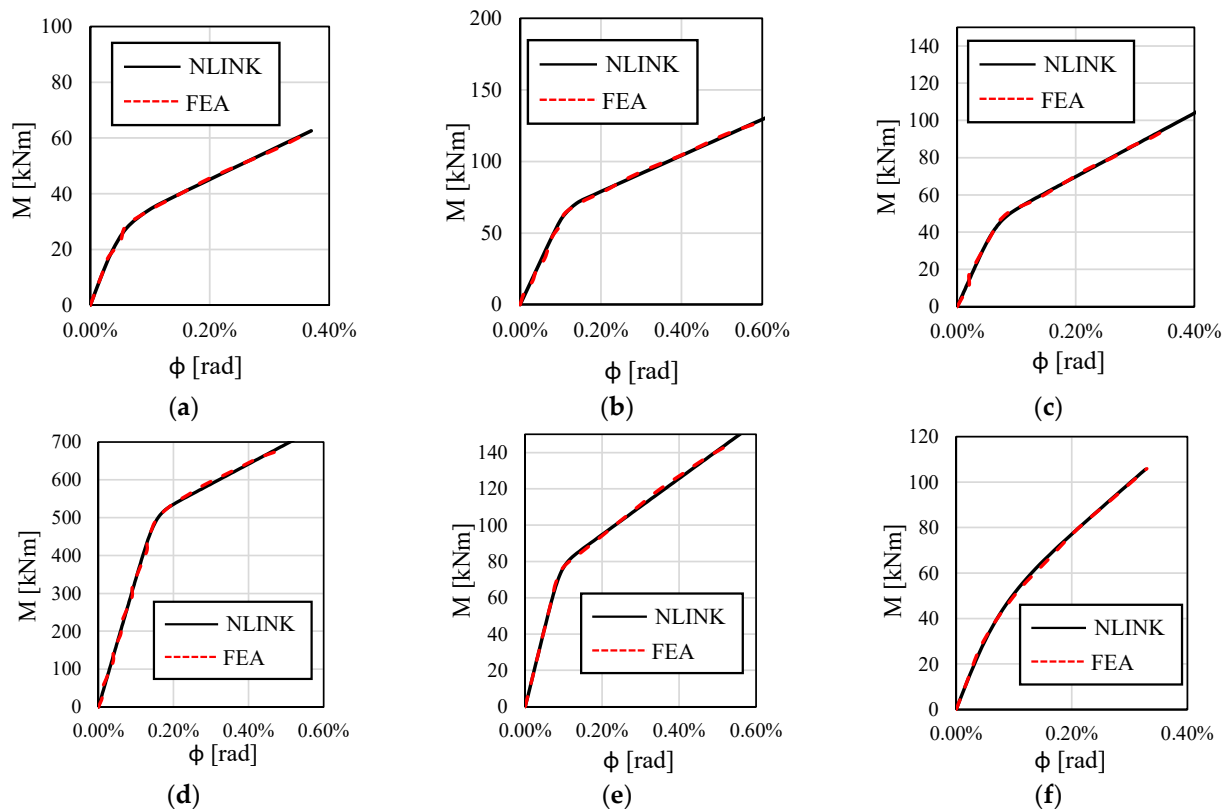


Figure 6. Non-linear link calibrations: (a) S-BO; (b) S-CH; (c) S-BS; (d) S-VT; (e) S-RC; and (f) S-PA.

4. Seismic Assessment of the Investigated Existing Buildings

4.1. Seismic Assessment Through Non-Linear Static Analysis

In compliance with both Italian and European standards [13–15], static non-linear (pushover) analyses were performed to evaluate the seismic performance of the structures studied, following a displacement-based approach. Various performance criteria were assessed in both the transverse and longitudinal directions for the limit states investigated.

In the longitudinal direction, where the lateral-force-resisting systems (LFRSs) were tension-only concentrically braced frames (CBFs), for the SD LS, the displacement demand (d_{Ed-SD}) was compared to the roof displacement corresponding to the local failure of the diagonals in tension (d_{Rd-SD}). Moreover, for the SD LS, it was required that the ratio between the displacement at the top of the column and the column height (story drift) be limited to less than 0.015 ($d_{Rd-SD-1.5\%}$), as specified by [29].

In the transverse direction, d_{Ed-SD} had to be less than the roof displacement (d_{Rd-SD}) corresponding to the rotational capacity of the flexural elements ($\theta_{Rd,SD}$), as defined in [27]. Additionally, the story drift was mandated to be less than 2% ($d_{Rd-SD-2.0\%}$) following the guidelines for MRF structures [29]. Furthermore, an additional local performance criterion was introduced for the second set of global models (the “R” configuration), focusing on the potential brittle failure of the column–base connections. For the Significant Damage (SD) limit state, the displacement demand (d_{Ed-SD}) was compared with the roof displacement at the point of local failure in a column–base connection ($d_{Rd-brit}$). Indeed, the calibrated non-linear link allowed us to quantify the bending moment demand in the joint ($M_{j,Ed}$) during the analyses up to failure ($M_{j,Ed} > M_{j,Rd}$).

With respect to the DL limit state, limiting the inter-story drift to less than 0.005 (corresponding roof displacement: $d_{Rd-DL-0.5\%}$) and preventing yielding in the lateral-force-resisting members (d_{Rd-DL}) were critical considerations. Local failures pertaining to chord-to-column connections or diagonal connections were not within the scope of this study. The influence of these local components on comprehensive seismic assessments was already discussed by the authors in a prior publication [30].

4.2. Results of Pushover Analyses in the Longitudinal Direction

Figure 7 illustrates the pushover curves derived for the six industrial buildings investigated in the longitudinal direction, accompanied by the capacity point, as defined by the aforementioned performance criteria. It is important to note that the modeling assumptions for the three sets of global models (i.e., I-R, R, and I-P) only concerned the behavior of the column–base joints in the transversal LFRSs. These assumptions do not affect the behavior in the longitudinal direction, and therefore, no significant differences were observed between the three model sets in this direction.

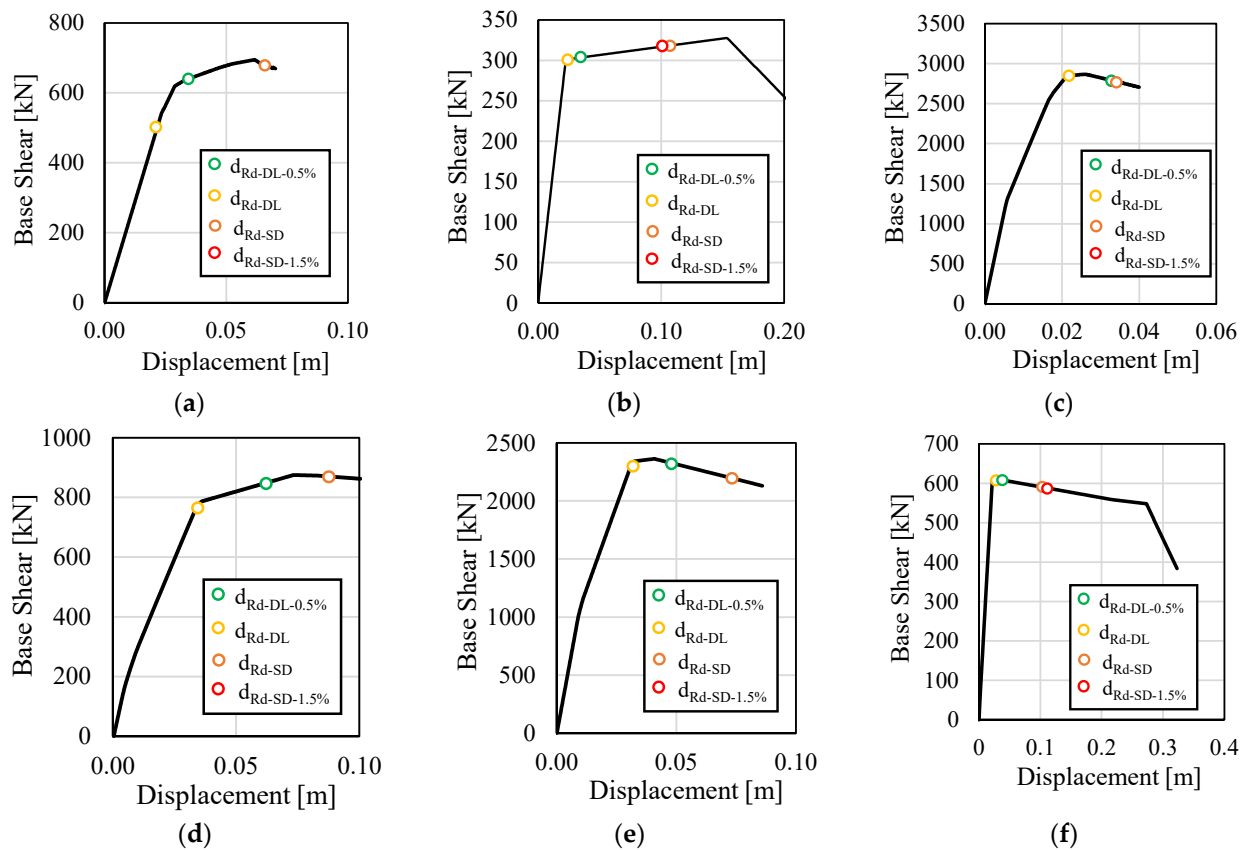


Figure 7. Pushover curves: (a) S-BO; (b) S-CH; (c) S-BS; (d) S-VT; (e) S-RC; and (f) S-PA.

As can be seen from Figure 7, the capacity of these structures in the DL state is constrained by local criteria regarding excessive deformation of the diagonals. The same consideration applies to the SD limit state, with the exception of S-CH, where the ultimate deformation of the diagonal occurs at an inter-story drift greater than 1.5%.

The idealized elastic–perfectly plastic base shear–roof displacement response was derived in compliance with [13,14,31] and subsequently depicted within the Acceleration–Displacement Response Spectrum (ADRS) framework with the demand spectrum in the DL and SD limit states. The displacement demands corresponding to the SD and DL limit states (d_{Ed-SD} and d_{Ed-DL} , respectively) were computed according to [32] and compared with the displacement capacity (d_{Rd-SD} , $d_{Rd-SD-1.5\%}$, d_{Rd-DL} , and $d_{Rd-DL-0.5\%}$) of the as-built structures.

To derive the “capacity spectrum” for a specific capacity point, it is necessary to identify the elastic displacement capacity beginning from the corresponding inelastic displacement. This process involves employing the equal displacement rule, adapted for short-period systems as per the modifications outlined in [32]. The safety indexes, defined as the ratio of the PGA of the capacity spectrum (PGA_C) to the PGA of the elastic demand spectrum (PGA_D) for the limit states investigated, are summarized in Tables 5 and 6.

Table 5. Longitudinal direction safety check for the SD LS.

Case Study ID	PGA_{D-SD} [m/s ²]	PGA_{C-SD} [m/s ²]	SD LS Ratio	$PGA_{C-SD-1.5\%}$ [m/s ²]	Ratio
-			-		-
S-BO	2.9	4.1	1.4	5.7	2.0
S-CH	2.9	6.3	2.2	6.0	2.1
S-BS	2.6	5.4	2.1	4.0	1.6
S-VT	2.6	4.6	1.8	/	/
S-RC	4.1	12.4	3.0	/	/
S-PA	3.0	8.6	2.8	9.0	3.0

Table 6. Longitudinal direction safety check for the DL LS.

Case Study ID	PGA_{D-DL} [m/s ²]	PGA_{C-DL} [m/s ²]	DL LS Ratio	$PGA_{C-DL-0.5\%}$ [m/s ²]	Ratio
-			-		-
S-BO	1.3	1.3	1.0	2.1	1.6
S-CH	1.3	1.4	1.1	2.2	1.7
S-BS	1.2	1.9	1.5	6.7	5.5
S-VT	1.2	1.9	1.6	3.1	2.6
S-RC	1.9	5.7	3.0	8.4	4.4
S-PA	1.3	3.1	2.3	3.4	2.6

Based on the findings presented in Tables 5 and 6, it is evident that the safety index assessed in the longitudinal direction exceeded 1.0 across all case studies for the limit states analyzed. They exhibit adequate stiffness and lateral resistance to seismic action.

4.3. Results of Pushover Analyses in the Transverse Direction

The same procedure as described earlier was employed to perform safety checks in the transverse direction. Here, the aim was to compare the response of the six industrial buildings by varying the base constraint conditions, considering an ideal condition (I-R and/or I-P), and a real condition (R), based on simulated designs and FEAs. In Figure 8, the pushover curves with their respective capacity points, as previously described, are depicted. Subsequently, in Tables 7 and 8, the safety indices in terms of the ratio between PGA_C and PGA_D are compared.

Unlike the behavior in the longitudinal direction, the curves shown in Figure 8 illustrate that the capacity of the analyzed structures in the transverse direction is limited by excessive lateral deformability. Locally, the members exceed the deformation limit at inter-story drift values higher than the established thresholds (i.e., 0.5% and 2.0% for DL and SD, respectively). However, when non-linear column–base joint behavior is explicitly accounted for, the seismic performance is primarily constrained by brittle failure of the base connections, particularly with reference to the SD limit state.

The results presented in Tables 7 and 8 illustrate the significant influence of the base connections. Specifically, concerning the SD verifications for the I-R configuration, there are no notable critical issues observed in either the rotational capacity checks of the flexural elements or those related to the maximum 2% IDR. Conversely, for the I-P configuration, the structure appears to be considerably more deformable, failing to meet the verifications regarding the maximum IDR for S-BO and S-RC. On the other hand, the findings for the R configuration indicate that the resistance capacity appears to be inadequate for the base connections of S-BO, S-BS, S-RC and S-PA, while due to the partial stiffness of the base connections, the verifications for the maximum IDR are not met for S-CH. The removal of the assumption of perfectly rigid base connections significantly impacts the verifications for the DL LS. In fact, in this scenario, for all case studies except for S-VT, the verifications are not satisfied when transitioning from the ideal I-R configuration to the real one.

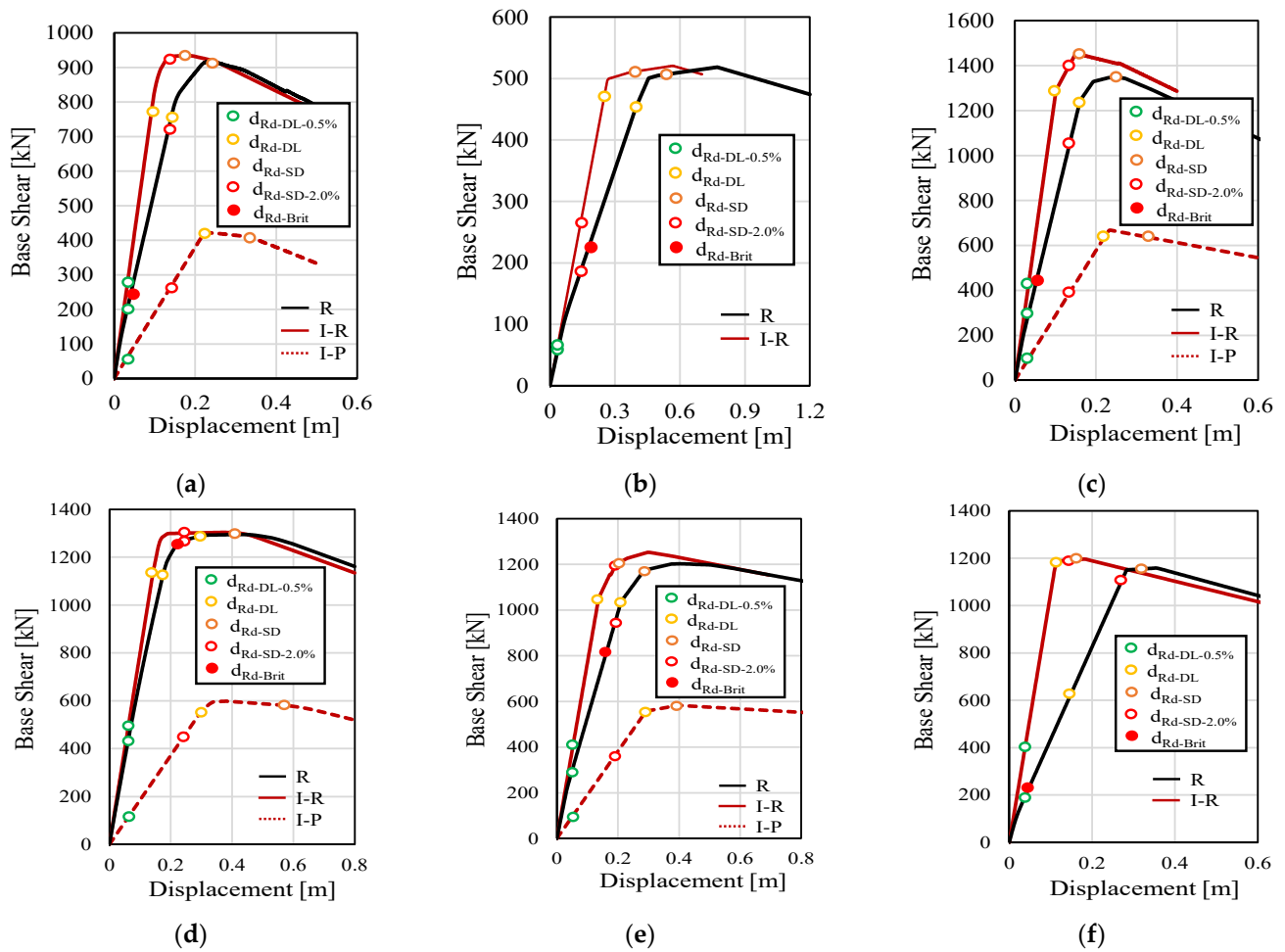


Figure 8. Pushover curves: (a) S-BO; (b) S-CH; (c) S-BS; (d) S-VT; (e) S-RC; and (f) S-PA.

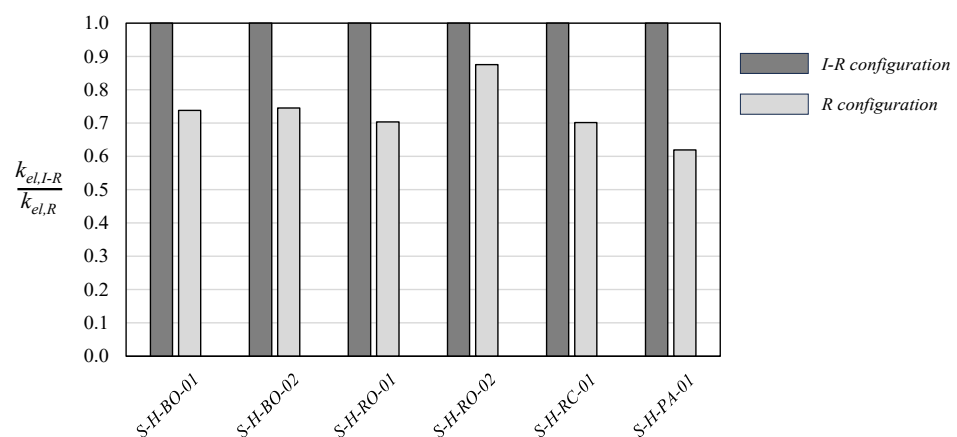
Table 7. Transverse direction safety checks for the SD LS.

Case Study ID	PGA _{D-SD} [m/s ²]	PGA _{C-SD} [m/s ²]	SD LS				
			Ratio	PGA _{C-SD-2.0%} [m/s ²]	Ratio	PGA _{C-SD-Brit} [m/s ²]	
S-BO-IR	2.9	5.5	1.9	4.6	1.6	/	/
S-BO-IP	2.9	5.0	1.7	2.4	0.8	/	/
S-BO-R	2.9	6.3	2.2	3.9	1.3	1.2	0.4
S-CH-IR	2.9	7.9	2.7	3.3	1.1	/	/
S-CH-R	2.9	9.6	3.4	2.7	0.9	3.7	1.3
S-BS-IR	2.6	6.5	2.5	5.4	2.1	/	/
S-BS-IP	2.6	6.4	2.5	2.5	1.0	/	/
S-BS-R	2.6	8.2	3.2	4.2	1.6	1.6	0.6
S-VT-IR	2.6	13.0	5.1	7.6	3.0	/	/
S-VT-IP	2.6	8.9	3.5	3.7	1.4	/	/
S-VT-R	2.6	8.6	3.4	7.0	2.7	6.5	2.5
S-RC-IR	4.1	5.0	1.2	4.9	1.2	/	/
S-RC-IP	4.1	5.0	1.2	3.0	0.7	/	/
S-RC-R	4.1	5.8	1.4	4.3	1.0	3.9	0.9
S-PA-IR	3.0	6.4	2.3	6.1	2.1	/	/
S-PA-R	3.0	8.3	2.7	4.4	1.4	1.8	0.6

Table 8. Transverse direction safety checks for the DL LS.

Case Study ID	PGA _{D-DL} [m/s ²]	PGA _{C-DL} [m/s ²]	DL LS Ratio	PGA _{C-DL-0.5%} [m/s ²]	Ratio
S-BO-IR	1.3	3.5	2.7	1.3	1.0
S-BO-IP	1.3	3.7	2.8	0.7	0.5
S-BO-R	1.3	3.9	3.0	1.1	0.8
S-CH-IR	1.3	5.7	4.4	0.9	0.7
S-CH-R	1.3	6.7	5.2	0.8	0.6
S-BS-IR	1.2	4.0	3.3	1.4	1.2
S-BS-IP	1.2	3.9	3.2	0.7	0.6
S-BS-R	1.2	5.1	4.2	1.1	0.9
S-VT-IR	1.2	4.4	3.6	1.9	1.6
S-VT-IP	1.2	4.5	3.8	1.2	1.0
S-VT-R	1.2	5.0	4.1	1.8	1.5
S-RC-IR	1.9	4.0	2.1	2.1	1.1
S-RC-IP	1.9	4.1	2.2	1.2	0.6
S-RC-R	1.9	4.6	2.4	1.7	0.9
S-PA-IR	1.3	5.3	4.0	2.2	1.6
S-PA-R	1.3	7.2	5.5	1.5	1.1

By analyzing the pushover curves, it is possible to compare the impact of column–base joint behavior on the overall lateral stiffness of the steel buildings examined. Specifically, Figure 9 illustrates the ratio between the elastic stiffness derived from non-linear static analyses assuming the ideal fully rigid column–base joint behavior ($k_{el,I-R}$) and the elastic stiffness from analyses where the moment–rotation behavior of the joints was explicitly modeled ($k_{el,R}$). The data in Figure 9 show that transitioning from the ideal to the actual joint behavior results in an average decrease in lateral stiffness of 30% for buildings with the RTF main frame typology, 35% for buildings with the PTF main frame typology, and 12% for buildings with the RPF main frame typology. These findings highlight the significant influence that realistic column–base joint behavior has on the structural performance of steel buildings.

**Figure 9.** Effect of the column–base joints on the overall lateral stiffness.

5. Seismic Strengthening Interventions

The pushover analysis results presented in the previous section emphasize the significant impact of explicitly modeling the column–base connections on the seismic response of single-story industrial buildings. In particular, for the “R” configuration, deficiencies were identified both locally in the SD limit state (with brittle failure of the connections) and globally in the DL limit state (overcoming the IDR threshold of 0.5%).

The conventional approach to improving a building's seismic performance involves adding lateral-force-resisting systems (LFRSs), such as exoskeletons or bracing systems, which can be effective but often involve high costs and a greater structural impact [30,33].

Alternatively, enhancing the column–base connections themselves offers a lower-cost, less intrusive solution. Specifically, stiffening of the column–base assembly with vertical stiffener plates and the addition of anchor rods can restore both its stiffness and strength. Studies have shown that improving the base connections can significantly improve both local and global seismic performance [34,35]. Strengthening these connections can reduce global deformability and maintain structural integrity under seismic loads. Additional research supporting this approach [36,37] demonstrates how targeted local retrofitting measures can yield significant improvements in the overall structural performance.

In this context, the proposed intervention involves reinforcing the column–base connections by adding vertical stiffener plates to increase the stiffness and anchor rods to improve the resistance. Strengthening interventions were applied to S-BO, S-BS, S-RC, and S-PA. However, as indicated in Tables 7 and 8, enhancing the column–base performance in terms of stiffness and resistance was insufficient to meet the code requirements for S-CH (refer to the I-R configuration in Tables 7 and 8). In this case, a global strengthening intervention is necessary to ensure compliance. The design of such global interventions is outside the scope of this research.

Figure 10 illustrates the detailed design of the local strengthening interventions.

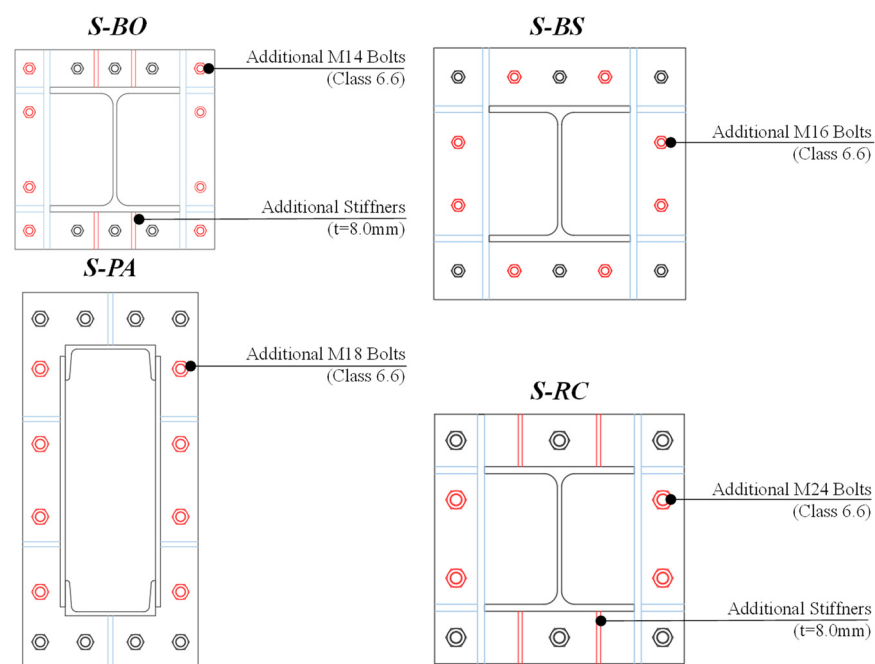


Figure 10. Local strengthening intervention.

The performance of the strengthened column–base connections was evaluated by implementing a 3D component-based finite element model (CBFEM) within the IDEA StatiCa environment, similar to the approach taken for the as-built connections. This modeling allowed for a detailed investigation of the connections' behavior, enabling an accurate comparison between the as-built and strengthened configurations (see Figure 11).

The expected bending moment demand at the column base was estimated for the I-R configuration by applying the N2 method to the pushover curve on the ADRS plan. By identifying the target displacement in the investigated limit state, it was possible to estimate the internal forces, including the bending moment and shear forces, at the column bases. This information provides for the design of additional anchor bolts and stiffeners to ensure that the column–base reinforcements meet the required strength and deformation capacities under seismic loading [22].

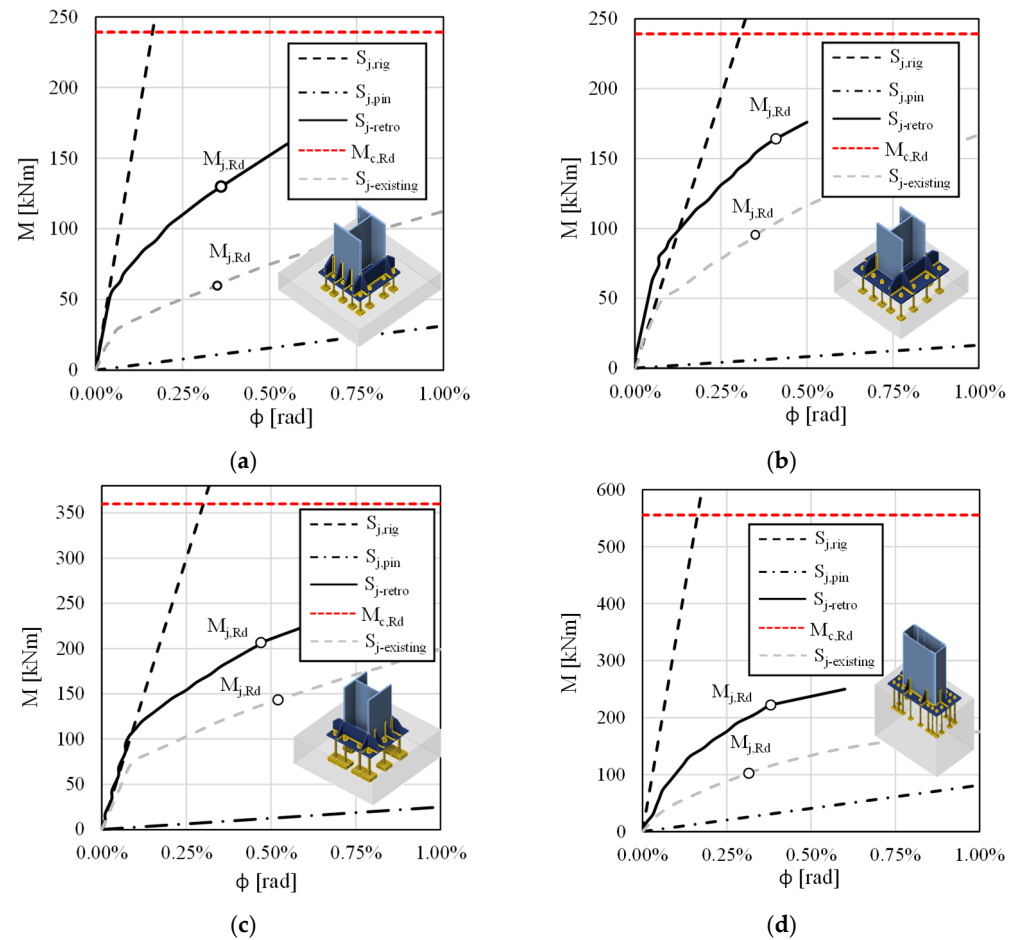


Figure 11. Moment–rotation response curves for strengthened column–base joints: (a) S-BO; (b) S-BS; (c) S-RC; and (d) S-PA.

The results shown in Figure 11 demonstrate the effectiveness of the strengthening interventions applied to the column–base connections. The enhancements provided notable increases in the moment resistance ($M_{j,Rd}$) of 109%, 73%, 44%, and 118% for S-BO, S-BS, S-RC, and S-PA, respectively. Additionally, the initial elastic stiffness of the connections improved significantly, with increases of 160%, 80%, 112%, and 46% for the same buildings.

To assess the implications of the local strengthening interventions on the global structural behavior, the column–base joints' local performance was incorporated into the global analyses. Therefore, non-linear links, properly calibrated for each intervention, were introduced into the 3D SAP2000 model to account for these modifications. Non-linear static analyses were conducted following the same assumptions as those used for the as-built configuration (R). The safety assessment for the retrofitted buildings (R-st) is summarized in Tables 9 and 10, which present the safety indexes, defined as the ratio of PGA_C to PGA_D for the limit states investigated.

Table 9. Transverse direction safety check in the SD LS.

Case Study ID	PGA_{D-SD} [m/s ²]	PGA_{C-SD} [m/s ²]	Ratio	SD LS		$PGA_{C-SD-Brit}$ [m/s ²]	Ratio
				$PGA_{C-SD-2.0\%}$ [m/s ²]	-		
S-BO-R-st	2.9	6.6	2.3	4.3	1.5	3.1	1.1
S-BS-R-st	2.6	7.8	3.0	4.5	1.7	2.7	1.0
S-RC-R-st	4.1	6.1	1.5	4.4	1.1	4.5	1.1
S-PA-R-st	3.0	8.4	2.8	5.5	1.8	3.2	1.1

Table 10. Transverse direction safety check in the DL LS.

Case Study ID	PGA_{D-DL} [m/s ²]	PGA_{C-DL} [m/s ²]	DL LS Ratio	$PGA_{C-DL-0.5\%}$ [m/s ²]	Ratio
-	-	-	-	-	-
S-BO-R-st	1.3	3.6	2.8	1.3	1.0
S-BS-R-st	1.2	5.1	4.2	1.2	1.0
S-RC-R-st	1.9	4.5	2.4	2.0	1.1
S-PA-R-st	1.3	7.0	5.4	1.8	1.4

As shown in Tables 9 and 10, the local strengthening interventions proposed allowed all the code requirements to be met in terms of both the local and global performance criteria for the limit states investigated. Indeed, in all the cases investigated, the seismic performance index exceeded 1, demonstrating the effectiveness of the retrofitting measures in enhancing the structural response. This approach, often overlooked, could offer an economical and effective retrofit solution without the need for more extensive LFRS additions.

6. Conclusions

This research underscores the importance of evaluating the seismic performance of existing strategic single-story steel buildings situated in Italy, with a particular emphasis on the nuanced behavior of column–base joints.

The methodology developed presents a systematic approach to assessing code-compliant seismic performance, taking into account the original design typologies and joint behaviors. From the results of numerical analyses, the following conclusions can be pointed out:

- The single-story steel buildings, although they were originally designed to consider gravity and wind loads only, demonstrate a satisfactory seismic performance in terms of lateral resistance and stiffness in the longitudinal direction.
- The absence of capacity design criteria in older regulations results in base nodes designed solely for resistance checks, categorized as semi-rigid and partial-strength according to the CBFEM analyses.
- The non-linear links introduced accurately replicate the local joint behavior in terms of the moment–rotation response, enabling the consideration of real joint performance in global 3D FEMs.
- In the transverse direction, the global structural behavior is heavily impacted by the base connections' performance. In most of the cases investigated, the joints show brittle behavior, mainly governed by the low resistance of the anchors. This local deficiency consistently precedes both the global structural ductility and the lateral deformability.
- The local strengthening at the column–base connections proposed offers an economical and effective retrofitting solution to improve both the local and global seismic performance. For brittle component failure, the seismic performance index increased from values between 0.4 and 0.9 to between 1.0 and 1.1. This corresponds to improvements ranging from 22% to 175%, ensuring compliance with the code prescriptions. In terms of lateral deformability check at DL limit state, the index increased from values between 0.8 and 1.1 to between 1.0 and 1.4, with improvements ranging from 11% to 27%.

Finally, the findings of this study are directly applicable to similar Italian single-story industrial buildings; however, the methodology for local and global assessment and retrofitting can be applied more broadly to various building types, especially those originally designed for gravity or wind loads. The approach provides a flexible framework that can be adapted to other structural configurations, making it relevant for a broader range of buildings beyond those considered in this study.

Author Contributions: Conceptualization, A.P. and R.T.; methodology, A.P. and R.T.; software, A.P. and R.T.; validation, A.P. and R.T.; formal analysis, A.P. and R.T.; investigation, A.P. and R.T.; resources, R.L.; data curation, A.P. and R.T.; writing—original draft preparation, A.P. and R.T.; writing—review and editing, R.T. and R.L.; visualization, A.P.; supervision, R.T. and R.L.; project administration, R.L. All authors have read and agreed to the published version of the manuscript.

Funding: This research received no external funding.

Data Availability Statement: The data are contained within the article.

Conflicts of Interest: The authors declare no conflicts of interest.

Nomenclature

List of symbols and acronyms

<i>ADRS</i>	Acceleration–Displacement Response Spectrum
a_g	Maximum horizontal acceleration on rigid ground, which has a 10% probability of being exceeded in 50 years
<i>C</i>	Seismic coefficient
<i>CBFEM</i>	Component-based finite element model
<i>CBFs</i>	Centrally braced frames
<i>CF</i>	Confidence factor
C_U	Utilization coefficient of a building
d_{Ed-DL}	Displacement demand in the DL limit state
d_{Ed-SD}	Displacement demand in the SD limit state
<i>DL</i>	Damage Limitation limit state
d_{Rd-DL}	Roof displacement corresponding to the first yielding of the steel members
$d_{Rd-DL-0.5\%}$	Roof displacement corresponding a story drift equal to 0.005
d_{Rd-SD}	Roof displacement corresponding to local failure of the steel members
$d_{Rd-SD-1.5\%}$	Roof displacement corresponding a story drift equal to 0.015
$d_{Rd-SD-2.0\%}$	Roof displacement corresponding a story drift equal to 0.02
F_E	Equivalent static seismic force according to the OS approach
<i>FEM</i>	Finite element method
F_w	Equivalent static wind force
f_y	Material yield strength assumed for a steel member's capacity (MPa)
$f_{y,m}$	Average value for the steel's yield strength (MPa)
<i>G</i>	Dead load (kN)
$g_{2k,c}$	Characteristic permanent load of lightweight claddings per unit area (kN/m ²)
$g_{2k,r}$	Characteristic permanent load of the roofing system per unit area (kN/m ²)
<i>GL</i>	Gravity load
<i>I</i>	Importance factor of a building
<i>IDR</i>	Inter-story drift ratio
<i>I-P</i>	Structural configuration considering pinned column–base joints
<i>I-R</i>	Structural configuration considering full-strength rigid column–base joints
$k_{el,I-R}$	Elastic stiffness derived from non-linear static analyses assuming the ideal fully rigid column–base joint behavior
$k_{el,R}$	Elastic stiffness from analyses where the moment–rotation behavior of a joint is explicitly modeled
<i>KL</i>	Knowledge Level
<i>LFRS</i>	Lateral-force-resisting system
<i>LS</i>	Limit state
$M_{c,Rd}$	Plastic bending capacity of a column
M_j	Bending moment acting at the column base
$M_{j,Rd}$	Bending capacity of the column–base joint
N_j	Axial force acting at the column base
<i>OS</i>	Obsolete seismic (design)
PGA_C	Peak ground acceleration of the capacity spectrum
PGA_D	Peak ground acceleration of the elastic demand spectrum
<i>PTFs</i>	Pinned truss frames

P_{VR}	Exceedance probability at V_R
R	Structural configuration considering the actual moment–rotation response of the column–base joint
R_d	Dynamic coefficient of a building
$RPFs$	Rigid portal frames
$R-st$	
$RTFs$	Rigid truss frames
$S-BO$	The steel single-story building located in Bologna (BO)
$S-BS$	The steel single-story building located in Brescia (BS)
$S-CH$	The steel single-story building located in Chieti (CH)
SD	Significant Damage limit state
S_j	Actual monotonic–moment rotation response of the column–base joint
$S_{j,pin}$	Upper bound of the moment–rotation response for a pinned column–base joint
$S_{j,rig}$	Lower bound of the moment–rotation response for the ideal fully rigid column–base joint
$S-PA$	The steel single-story building located in Palermo (PA)
$S-RC$	The steel single-story building located in Reggio Calabria (RC)
$S-VT$	The steel single-story building located in Viterbo (VT)
T_R	Mean return period of the seismic action employed
V_j	Shear acting at the column base
V_N	Nominal design life of a building
V_R	Reference period
W_{Tot}	Seismic weight of a building
$\theta_{Rd,SD}$	Rotational capacity of the flexural elements

References

1. National Institute of Statistics (ISTAT). *16° Censimento Generale della Popolazione e delle Abitazioni*; National Institute of Statistics (ISTAT): Rome, Italy, 2021. (In Italian)
2. Dall’Asta, A.; Landolfo, R.; Salvatore, W. *Edifici Monopiano in Acciaio ad Uso Industriale*; Dario Flaccovio Editore: Palermo, Italy, 2022. (In Italian)
3. Landolfo, R.; Fomisano, A.; Di Lorenzo, G.; Di Filippo, A. Classification of european building stock in technological and typological classes. *J. Build. Eng.* **2022**, *45*, 103482. [[CrossRef](#)]
4. Tsavdaridis, K.-D. Strengthening Techniques: Code-Deficient Steel Buildings. In *Encyclopedia of Earthquake Engineering*; Springer: Berlin/Heidelberg, Germany, 2014. [[CrossRef](#)]
5. *RD 18/04/1939 n. 2229*; Norme per la Esecuzione delle Opere in Conglomerate Cementizio Semplice ed Armato. Gazzetta Ufficiale della Repubblica Italiana n. 92: Rome, Italy, 1940. (In Italian)
6. *D.M. 30/05/1974*; Norme Tecniche per la Esecuzione delle Opere in Cemento Armato Normale e Precompresso e per le Strutture Metalliche. Gazzetta Ufficiale della Repubblica Italiana n. 198: Rome, Italy, 1974. (In Italian)
7. *D.M. 26/03/1980*; Norme Tecniche per la Esecuzione delle Opere in Cemento Armato Normale e Precompresso e per le Strutture Metalliche. Gazzetta Ufficiale della Repubblica Italiana n. 176: Rome, Italy, 1980. (In Italian)
8. *D.M. 25/07/1985*; Norme Tecniche per la Esecuzione delle Opere in Cemento Armato Normale e Precompresso e per le Strutture Metalliche. Gazzetta Ufficiale della Repubblica Italiana n. 113: Rome, Italy, 1986. (In Italian)
9. *RD 25/03/1935 n. 640*; Nuovo Testa Delle Norme Tecniche di Edilizia con Speciali Prescrizioni per le Località Colpite dai Terremoti. Gazzetta Ufficiale della Repubblica Italiana n. 640: Rome, Italy, 1935. (In Italian)
10. *DM. 03/03/1975*; Approvazione delle Norme Tecniche per le Costruzioni in Zone Sismiche. Gazzetta Ufficiale della Repubblica Italiana n. 93: Rome, Italy, 1975. (In Italian)
11. CNR (Consiglio Nazionale delle Ricerche). *CNR-UNI 10011: Steel Structure—Instruction for Design, Construction, Testing and Maintenance*; Consiglio Nazionale delle Ricerche: Rome, Italy, 1967. (In Italian)
12. CNR (Consiglio Nazionale delle Ricerche). *CNR-UNI 10012: Ipotesi di Carico Sulle Costruzioni*; Consiglio Nazionale delle Ricerche: Rome, Italy, 1967. (In Italian)
13. *D.M. 17/01/2018*; Aggiornamento delle Norme Tecniche per le Costruzioni. Gazzetta Ufficiale della Repubblica Italiana n. 42: Rome, Italy, 2018. (In Italian)
14. *C.S.LL.PP., Circolare n.7 21/01/2019*; Istruzioni per L’applicazione dell’«Aggiornamento delle “Norme tecniche per le Costruzioni”». Gazzetta Ufficiale della Repubblica Italiana n. 5: Rome, Italy, 2019. (In Italian)
15. CEN (European Committee for Normalization). *EN1998:3 Eurocode 8: Design of Structures for Earthquake Resistance—Part 3: Assessment and Retrofitting of Buildings*; European Committee for Normalization: Brussels, Belgium, 2005.

16. Di Lorenzo, G.; Formisano, A.; Terracciano, G.; Landolfo, R. Iron alloys and structural steels from XIX century until today: Evolution of mechanical properties and proposal of a rapid identification method. *Constr. Build. Mater.* **2021**, *302*, 124132. [[CrossRef](#)]
17. CEN (European Committee for Normalization). *UNI EN 10025-1: Hot Rolled Products of Structural Steels—Part 1: General Technical Delivery Conditions*; European Committee for Normalization: Brussels, Belgium, 2005.
18. da Silva, L.S.; Rebelo, C.; Nethercot, D.; Marques, L.; Simoes, R.; Vila Real, P.M.M. Statistical evaluation of the lateral–torsional buckling resistance of steel I-beams, Part 2: Variability of Steel properties. *J. Constr. Steel Res.* **2009**, *65*, 832–849. [[CrossRef](#)]
19. CEN (European Committee for Normalization). *EN1998-1: Eurocode 8: Earthquake Resistance Design of Structures*; European Committee for Normalization: Brussels, Belgium, 2005.
20. ASCE (American Society of Civil Engineers). *Technical Council on Lifeline Earthquake Engineering. Northridge Earthquake—Lifeline Performance and Post-Earthquake Response, Monograph No. 8 1995*; American Society of Civil Engineers: New York, NY, USA, 1995.
21. Northridge Reconnaissance Team. Earthquake Spectra, Northridge Earthquake of January 17, 1994. *Reconnaiss. Rep. Suppl. C-2 1996*, *11*, 25–47.
22. CEN (European Committee for Normalization). *EN1993:1-8 Eurocode 3: Design of Steel Structures—Part 1–8: Design of Joints*; European Committee for Normalization: Brussels, Belgium, 2005.
23. Danieli, D.; De Miranda, F. *Strutture in Acciaio per L'edilizia Civile e Industriale, Collana Tecnico Scientifica per la Progettazione Delle Strutture in Acciaio*; Italsider S.p.A.: Genova, Italy, 1971. (In Italian)
24. Della Corte, G.; Cantisani, G. Modelling of colum base plate connections with palet stiffeners and non-proportional loading. *Proc. Civ. Eng.* **2023**, *6*, 1305–1311.
25. IDEA StatiCa. Connection Design 2023. Available online: <https://www.ideastatica.com/> (accessed on 3 October 2024).
26. Computers and Structures Inc. (CSI). *SAP2000 Integrated Software for Structural Analysis and Design*; Computers and Structures Inc.: Berkeley, CA, USA, 2024.
27. ASCE (American Society of Civil Engineers). *ASCE/SEI 41-17: Seismic Evaluation and Retrofit of Existing Buildings*; American Society of Civil Engineers: Reston, VA, USA, 2018.
28. Wen, Y.K. Method for Random Vibration of Hysteretic Systems. *ASCE J. Engng. Mech.* **1976**, *102*, 249–263. [[CrossRef](#)]
29. CEN/TC 250/SC 8, prEN1998-1-2 SC8 15-03-2022: *Eurocode 8: Earthquake Resistance Design of Structures (2022 Draft)*; European Committee for Normalization: Brussels, Belgium, 2022.
30. Tartaglia, R.; Milone, A.; Prota, A.; Landolfo, R. Seismic retrofitting of existing industrial steel buildings: A case-study. *Materials* **2022**, *15*, 3276. [[CrossRef](#)] [[PubMed](#)]
31. Fajfar, P. A nonlinear analysis method for performance-based seismic design. *Earthq. Spectra* **2000**, *16*, 573–592. [[CrossRef](#)]
32. Vidic, T.; Fajfar, P.; Fischinger, M. Consistent inelastic design spectra: Strength and displacement. *Earthq. Eng. Struct. Dyn.* **1994**, *23*, 507–521. [[CrossRef](#)]
33. Di Lorenzo, G.; Tartaglia, R.; Prota, A.; Landolfo, R. Design procedure for orthogonal steel exoskeleton structures for seismic strengthening. *Eng. Struct.* **2023**, *275*, 115252. [[CrossRef](#)]
34. Zareian, F.; Kanvide, A. Effect of column-base flexibility on the seismic response and safety of steel moment-resisting frames. *Earthq. Spectra* **2013**, *29*, 1537–1559. [[CrossRef](#)]
35. Lin, K.S.; Kurata, M.; Kawasaki, Y.; Kitatani, Y. Investigation of low-disturbance seismic retrofit method for steel column bases using curved members. *Jpn. Archit. Rev.* **2023**, *7*, e12429. [[CrossRef](#)]
36. Aichouche, M.; Abidelah, A.; Bouchair, A.; Kerdal, D.; Seghir, A.; Vatansever, C. Effects of stiffeners on anchor rod flexural strength in column base-plate connections. *J. Constr. Steel Res.* **2024**, *222*, 108983. [[CrossRef](#)]
37. Mehdi, B.; Boumechra, N.; Missoum, A.; Bouchair, A. Connection of a Steel Column Base Plate: Mechanical Behavior and Stiffening Effects. *Civ. Eng. J.* **2022**, *8*, 1764–1786. [[CrossRef](#)]

Disclaimer/Publisher’s Note: The statements, opinions and data contained in all publications are solely those of the individual author(s) and contributor(s) and not of MDPI and/or the editor(s). MDPI and/or the editor(s) disclaim responsibility for any injury to people or property resulting from any ideas, methods, instructions or products referred to in the content.